Supporting Information

Early Transition Metal Nano-carbides and Nano-hydrides from Solid-State Metathesis initiated at Room Temperature

Rémi F. André,[1] Florian D'Accriscio,[1] Alexy P. Freitas,[1] Guillaume Crochet,[1] Corinne Bouillet,[2] Mounib Bahri,[2], Ovidiu Ersen,[2] Clément Sanchez,[1] Sophie Carenco,[1,]*

[1] Sorbonne Université, CNRS, Collège de France, Laboratoire de Chimie de la Matière Condensée de Paris (LCMCP), 4 place Jussieu, 75005 Paris, France

[2] Institut de Physique et Chimie des Matériaux de Strasbourg (IPCMS), UMR 7504 CNRS-Université de Strasbourg, 23 rue du Loess, 67034 Strasbourg Cedex 2, France

*Corresponding author. E-mail: sophie.carenco@sorbonne-universite.fr

Table of contents

A. General procedures and Materials and Methods

A.1. Materials and methods

All experiments and manipulations were carried out under an atmosphere of dry nitrogen using standard Schlenk techniques or in an argon-filled glovebox, if not otherwise stated. Nanoparticles isolation was performed at ambient atmosphere. $NbCl_5$ (99.9 %), WCl_6 (99.9 %) and K (99.5 %) were purchased from Sigma-Aldrich. Ethanol (96 %) was purchased from VWR. $ZrCl_4$ (99.5 %) was purchased from Strem Chemicals. $HfCl_4$ (99.9 %), $MoCl_5$ (99.6 %), $TaCl_5$ (99.8 %), carbon black acetylene (50 % compressed, 99.9 % purity) and graphite powder were purchased from Alfa Aesar.

Purification by recrystallization of WCl_6

Commercial WCl_6 is contaminated with traces of metallic W(0). It was purified by recrystallization in a Schlenk tube under static vacuum at 210 °C during 2 h. The solid at the bottom of the Schlenk gradually sublimes (red gas phase) and recrystallizes as big violet crystals on the glass walls in the cold part of the Schlenk.

Synthesis of KC_4 and KC_8

[Caution, the final compounds KC_4 and KC_8 are pyrophoric]

In a Schlenk tube and in glovebox, 1 g of metallic potassium cut in pieces (25.57 mmol, 1 equiv.) and 2.46 g of dry graphite (204.56 mmol, 8 equiv.) were mixed with a stirrer bar. The tube is put under static vacuum and heated with a heat gun under vigorous magnetic agitation for at least 1 h in order to obtain a homogeneous powder. Metallic potassium melts and is incorporated into the carbon phase to form a bronze powder KC_8. The obtained powder (100 % yield) was then stored under inert atmosphere for up to several weeks, it starts to degrade after two months. A too high

temperature may result in the sublimation and resolidification of potassium on the walls of the Schlenk which forms iridescences. The same procedure was followed to impregnate acetylene black (ac-C, KC_4) with 1.23 g of dry acetylene black 50 % compressed (102.28 mmol, 4 equiv.) for 1 g of potassium. The material remained black in this case.

Synthesis of nanoparticles

Caution! Most solid-state metathesis reactions are highly exothermic, and in some cases the precursors may spontaneously detonate when mixed or ground together. Care should be taken to do reactions of this type on a small scale with adequate safety precautions. These reactions may ignite when exposed to small amounts (one drop) of a solvent. The synthesis was adapted from a previous paper.[1]

The protocol is described in the experimental section of the main article.

A.2. Characterizations

X-ray diffraction on powders

X-ray diffraction patterns of dry powders were measured on a Bruker D8 diffractometer using Cu Kα radiation at 1.5406 Å (and Mo Kα radiation at 0.7093 Å for measurements in capillary). Typical diffractograms were collected with steps of 0.05 ° and a scanning speed of 3 s/point. Backgrounds of the patterns are subtracted and heights of the samples are corrected (KCl was used as an internal reference) using the EVA software.

The reference patterns Powder Diffraction File are: KCl [00-041-1476], Zr [04-008-1477], ZrC [00-035-0784], ZrH_2 [00-017-0314], ZrO_2 [04-007-0952], Hf [00-038-1478], $HfH_{1.74}$ [00-005-0641], HfO_2 [00-053-0560], Nb [00-034-0370], Nb_6C_5 [04-007-6990], $NbH0_{.8}$ [01-081-6188], Ta [00-004-0788], TaC [00-035-0801], Ta_2H [00-032-1281], Mo [04-014-7435], Mo_2C [04-001-2996], W [00-004-0806], W_2C [04-014-5679], WC [00-051-0939].

For the determination of the relative proportions of the different phases in the pie charts, we relied on the respective surface of the main peaks for all the phases: 38.5 ° for Nb(0), {34.8 °, 40.4 °} for Nb_6C_5, 37.1 ° for $NbH_{0.8}$, {34.5 °, 40.5 °} for TaC, 37.6 ° for $TaH_{0.5}$, 40.5 ° for Mo(0), {34.3 °, 38.0 °, 39.4 °} for Mo_2C, 40.6 ° for W(0) and {34.6 °, 38.0 °, 39.6 °} for W_2C. As much as possible, we used FullProf software to model the different peaks but for the most complex cases, the estimation was done visually. When one of these peaks could not be distinguished from the diffraction peak of KCl at 40.5 °, we estimated the surface to be removed (one third of the KCl diffraction peak at 28.3 °).

Transmission electronic microscopy

For TEM analysis, a drop of a diluted solution of nanos dispersed in ethanol or hexanes was allowed to dry on an amorphous carbon coated copper grid. TEM images were collected with a TWIN 120 (TECNAI SPIRIT) at 120 kV. STEM bright field (BF) and high angle annular dark field (HAADF) images were acquired using a probe corrector Cs JEOL 2100F microscope operating at 200 kV.

XPS spectroscopy

XPS Spectra were collected on an Omicron Argus X-ray photoelectron spectrometer, using a monochromated Al K_α ($h\upsilon$= 1486.6 eV) radiation source having a 300 W electron beam power. The samples were analyzed under ultra-high-vacuum conditions (10^{-8} Pa). After recording a broad range spectrum (pass energy, 100 eV), high-resolution spectra were recorded for the C 1s, O 1s, Zr 3d, Nb 3d, Mo 3d, Hf 4d, Hf 4f, W 4d and W 4f core XPS levels (pass energy, 20 eV). We found evidence of remaining KCl : next to C 1s we found signal from K 2p (between 293 and 297 eV), next to Nb 3d and Hf 4d we found signal from Cl 2p (between 197 and 201 eV) and next to W 4d we found signal from Cl 2s (between 268 and 270 eV). The binding energies were calibrated with respect to the C 1s peak at 284.5 eV (mainly graphitic carbon). Spectrum processing was carried out using the CasaXPS software package.

Mo K-edge XANES spectroscopy

Mo K-edge XANES data were collected in the ROCK beamline at SOLEIL, at an electron energy of 2.7 GeV and an average ring current of 450 mA. The incoming photons were selected with a Si (220) double-crystal monochromator. A 6 mg portion of the sample was diluted in *ca.* 55 mg of graphite and was compressed to form a 10 mm diameter pellet. Spectrum processing was carried out using the Athena software.

B. Supplementary data

B.1. Literature review

Ref.	Precursor	Reduction agent	Product	Ignition temperature if SSM	Temperature and time of reaction	NP size (nm)	Comments
[2]	$TiCl_3$, VCl_3, $ZrCl_4$, $MoCl_3$, $MoCl_5$, WCl_4	Al_4C_3	TiC, V_8C_7, ZrC, Mo_2C, WC (traces of Mo and W_2C)	No solid flame observed	Up to 1000 °C + 2-5 days	30 to 70	Under vacuum in sealed ampoule
		CaC_2		200-350 °C[1]	Up to 500 °C + 1 hour		
[3]	$TiCl_3$, VCl_3, $CrCl_2$, $CrCl_3$ $ZrCl_4$, $NbCl_5$, $MoCl_3$, $HfCl_4$, $TaCl_5$, WCl_4	Al_4C_3	TiC, V_8C_7, Cr_3C_2, ZrC, NbC, Mo_2C, HfC, TaC, WC (traces of Mo and W_2C)	No solid flame observed	Up to 1000 °C + 1 h	10 to 30	Under vacuum in sealed ampoule
		CaC_2		*n.a.*	*n.a.*	10 to 30	Electric filament initiation (1000 °C) in a ceramic boat in air
				200-350 °C	Up to 500 °C + 1 h	10 to 30	Under vacuum in sealed ampoule
[4]	V_2O_3, $NaVO_3$, Nb_2O_5, $LiNbO_3$, Ta_2O_5, $LiTaO_3$, MoO_3, Li_2MoO_4, Li_2WO_4	CaC_2	V_8C_7, NbC, TaC, Mo_2C, WC	480-650 °C[2]	Up to 1000 °C + 12 h[3]	10 to 40	Under vacuum in sealed ampoule[4]
		SrC_2					
[1]	$TiCl_4$, VCl_4	KC_2-KC_4-KC_8	TiC, VC	20 °C	*n.a.*	5 to 30	Liquid metal chlorides
	$MoCl_5$, WCl_6		Mo_2C, W_2C	< 75 °C			Under Ar
This work	$ZrCl_4$, $NbCl_5$, $MoCl_5$, $HfCl_4$, $TaCl_5$, WCl_6	KC_4-KC_8	Zr, ZrC, Nb, Nb_6C_5, Mo, Mo_2C, Hf, Ta, TaC, W, W_2C	20-75 °C	*n.a.*	5 to 50	Under vacuum or in Ar
			ZrH_2, $NbH_{0.8}$, HfH_2, Ta_2H				After neutralization with $EtOH/H_2O$
[5]	$TiCl_4$, VCl_3, $ZrCl_4$, $NbCl_5$, $HfCl_4$, $TaCl_5$	n-BuLi	TiC, V_4C_3, ZrC, NbC, HfC, TaC	*n.a.*	r.t then 1000 °C + 1-12 h	5 to 50	In hexane to form colloid precursors, followed by annealing step in vacuum
[6]	$NbCl_5$	Li_2C_2	Nb or Nb_6C_5	*n.a.*	Up to 600 °C + 10 h		Different thermal events between 150 °C and 600 °C but none corresponding to an SSM

[1] CaC_2 undergoes a phase change at 350 °C, otherwise the reaction occurs at the melting point of the metal halide salt
[2] No thermal flash was observed as for metal halides but a darkening in 20-30 s of the powder instead
[3] The annealing during 12 h proved to be necessary as more crystalline products were obtained
[4] Reaction initiated at room temperature with a hot filament failed to propagate

Ref.	Precursor	Reduction agent	Product	Ignition temperature if SSM	Temperature and time of reaction	NP size (nm)	Comments
[7]	$TiCl_4$	CaC_2	TiC	*n.a.*	500 °C + 8 h	40	In autoclave
[8]	$NbCl_5$	CaC_2	NbC	*n.a.*	r.t. during 15 min	50	Mechanochemical processing (high energy milling)
[9]	TiO_2, V_2O_5, MoO_3	CaC_2 and Mg	TiC, V_2C, Mo_2C	*n.a.*	600 °C + 10 h	30	Mg-assisted reduction, in autoclave with Li_2CO_3
[10]	ZrO_2	Mg	ZrC	*n.a.*	600 °C + 20 h	30	Mg-assisted reduction, in autoclave with Li_2CO_3
[11]	HfO_2	Mg	HfC	*n.a.*	700 °C + 10 h	10	Mg-assisted reduction, in autoclave with Li_2CO_3
[12]	WO_3	Mg and EtOH	WC	*n.a.*	600 °C + 15 h	100 to 200	Mg-assisted reduction, in autoclave with ethanol
[13]	V_2O_5, Nb_2O_5, MoO_3, Ta_2O_5, WO_3	Melamine	VC, NbC, MoC, TaC, WC	*n.a.*	Up to 1100 °C + 30 min	7 to 18	Reagents pressed in a pellet and reaction under vacuum in sealed ampoule
[14]	V_2O_5, Nb_2O_5, Ta_2O_5, WO_3	Cyanamide	VC, NbC, TaC, WC	*n.a.*	Up to 1150 °C + 30 min	6 to 35	Reagents pressed in a pellet and reaction under vacuum in sealed ampoule

Table S1: Selection of works on the synthesis of metal carbide nanoparticles. SSM only fits for this work and references [1-4].

B.2. Photos and snapshots of videos

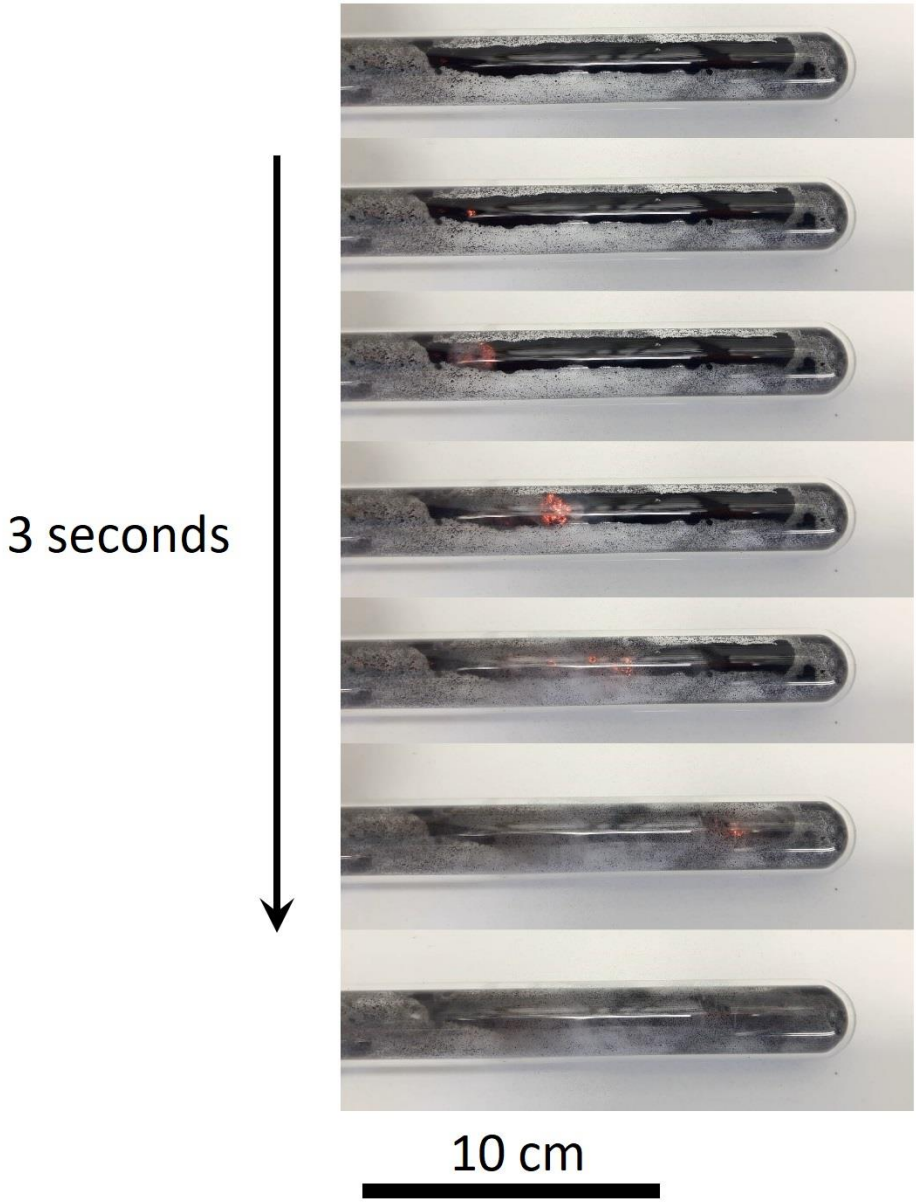

Figure S1: A sequence of photographs showing the ignition and reaction stage of a SSM reaction between $ZrCl_4$ + 4 KC_4 under Ar, covering a time span of about 3 seconds. The reaction was initiated through external heating by using a heat gun.

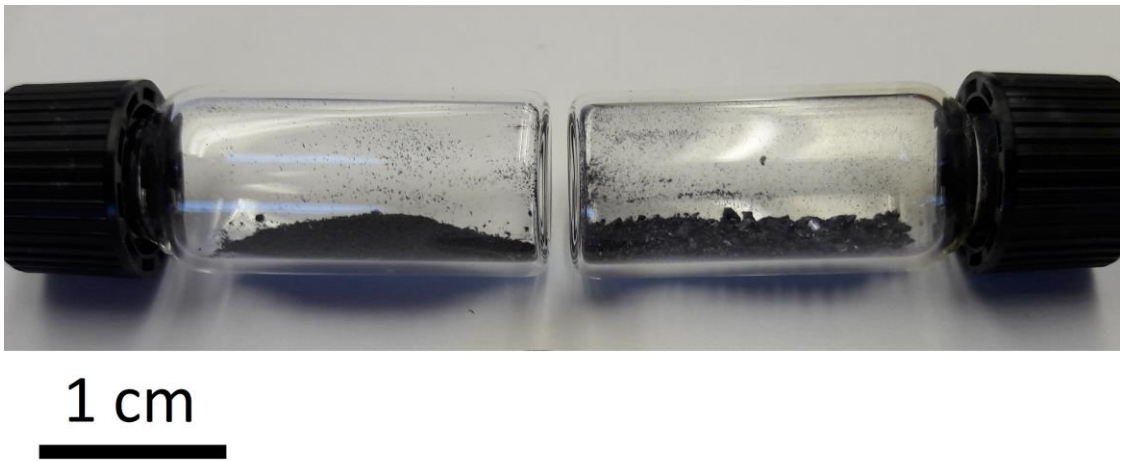

Figure S2: Photo of the precursor WCl_6 before (left) and after (right) recrystallization.

B.3. Thermodynamic data and calculations

Unless otherwise stated, all the thermodynamical data are from the Thermodynamical tables of the NIST-JANAF.[15]

The released energy by the reaction corresponds to the absolute value of the enthalpy of reaction, determined via Hess's law.

For instance, for the reaction with $ZrCl_4$:

$$ZrCl_4 + 4\,KC_4 \rightarrow Zr(0) + 4\,KCl + 16\,C$$

$$\Delta_{\text{reaction}}\text{H°} = \Delta_{\text{f}}\text{H°(Zr)} + 4\,\Delta_{\text{f}}\text{H°(KCl)} + 16\,\Delta_{\text{f}}\text{H°(C)} - (\Delta_{\text{f}}\text{H°}(\text{ZrCl}_4) + 4\,\Delta_{\text{f}}\text{H°}(\text{KC}_4))$$

By definition, the enthalpy of formation of Zr(0) and graphite is zero.

$$\Delta_{\text{reaction}}\text{H° (kJ/mol)} = 4\,(-436.7) - (-980.5 + 4\,(-30.9)) = -642.7$$

Compounds	Enthalpy of formation (kJ/mol)	Compounds	Enthalpy of formation (kJ/mol)
Chlorides		**Oxides**	
$ScCl_3$	-944.8		
YCl_3	-982.4		
$LaCl_3$	-1070.7		
$TiCl_3$	-721.7		
$ZrCl_4$	-980.5	**ZrO_2**	-1097.5
$HfCl_4$	-990	**HfO_2**	*no data*
VCl_3	-580.7		
$NbCl_5$	-797.5	**Nb_2O_5**	-1899.5
$TaCl_5$	-859	**Ta_2O_5**	-2046
$CrCl_2$	-395.4		
$CrCl_3$	-556.5		
$MoCl_3$	-393	**MoO_2**	-587.9
$MoCl_5$	-527.2	**MoO_3**	-745.2
WCl_4	-443.1		
WCl_6	-593.7	**WO_3**	-842.9
$MnCl_2$	-481.2		
$FeCl_2$	-341.7		
$FeCl_3$	-399.2		
$CoCl_2$	-312.5		
$NiCl_2$	-304		
Alkaline derivatives			
KC_4	-30.9	**KCl**	-436.7
KC_8	-33.4	**K_2O**	-363.2
CaC_2	-62.8	**$CaCl_2$**	-795.8
		CaO	-635.7
SrC_2	-60	**$SrCl_2$**	-828.8
		SrO	-592

Table S2. List of enthalpies of formation of the different relevant compounds.

Heat capacity of solid KCl as a function of reduced temperature t (t=T(K)/1000) in J/mol/K:

$$C_p(KCl) = 35.41 + 70.03\,t - 91.38\,t^2 + 52.52\,t^3 + 0.1534\,t^{-2}$$

KCl melts at 770 °C (1043 K) with a standard fusion enthalpy of 25.5 kJ/mol.

Liquid KCl heat capacity is estimated constant at 73.6 J/mol/K.

KCl boils at 1500 °C (1773 K) with a standard evaporation enthalpy of 162.4 kJ/mol.

Heat capacity of solid $CaCl_2$ as a function of reduced temperature t in J/mol/K:

$$C_p(CaCl2) = 87.30 - 35.08\,t + 44.13\,t^2 - 9.85\,t^3 - 0.6742\,t^{-2}$$

$CaCl_2$ melts at 772 °C (1045 K) with a standard fusion enthalpy of 28.5 kJ/mol.

Liquid $CaCl_2$ heat capacity is estimated constant at 102.5 J/mol/K.

$CaCl_2$ boils at 1935 °C (2208 K).

Heat capacity of graphite as a function of reduced temperature t in J/mol/ K[16]:

$$C_p(graphite) = 27.02 + 0.0457\,t - 4.528\,t^{-1} - 2.179\,t^{-2} + 0.7991\,t^{-3} - 0.07207t^{-4}$$

Heat capacity of metal (very close values for all the metals studied here, based on Tantalum) as a function of reduced temperature t in J/mol/K:

$$C_p(metal) = 20.69 + 17.29\,t - 15.68\,t^2 + 5.608\,t^3 + 0.06158\,t^{-2}$$

Pyrex glass has a heat capacity of 0.75 J/g/K which corresponds to a heat capacity of 7.5 J/K for the 10 g of the glass walls of the Schlenk tube near the powder. The auto-initiated reaction with WCl_6 released 300 J which would correspond to a final elevation of 45 °C of the part of the vessel in contact with the reaction. This order of magnitude is coherent with the feeling of heat with hand (clearly much hotter than before the reaction without being burning).

Starting material	**Enthalpy of reaction per atom of transition metal (kJ/mol)**			
	Reduction by KC_4	Reduction by KC_8	Reduction by CaC_2	Reduction by SrC_2
Chlorides				
$TiCl_3$	-496	-488	-378	-432
$ZrCl_4$	-642	-632	-485	-557
$HfCl_4$	-633	-623	-476	-548
VCl_3	-637	-629	-519	-573
$NbCl_5$	-1231	-1219	-1035	-1125
$TaCl_5$	-1170	-1157	-974	-1063
$CrCl_2$	-416	-411	-338	-373
$CrCl_3$	-661	-653	-543	-597
$MoCl_3$	-824	-817	-707	-760
$MoCl_5$	-1502	-1489	-1305	-1395
WCl_4	-1180	-1170	-1023	-1095
WCl_6	-1841	-1826	-1605	-1713
$ScCl_3$		-272		
YCl_3		-235		
$LaCl_3$		-147		
$MnCl_2$		-330		
$FeCl_2$		-470		
$FeCl_3$		-818		
$CoCl_2$		-499		
$NiCl_2$		-507		
Oxides				
ZrO_2	495	505	-48	34
HfO_2	*n.d.*	*n.d.*	*n.d.*	*n.d.*
Nb_2O_5	197	197	-482	-380
Ta_2O_5	270	282	-409	-307
MoO_2	-15	-5	-558	-476
MoO_3	-160	-144	-974	-851
WO_3	-61	-46	-876	-753

Table S3. List of enthalpies of reaction for SSM and MSSM reactions.

Starting material	**Adiabatic temperature T_{ad}**		
	Reduction by KC_4	Reduction by KC_8	Reduction by CaC_2
$TiCl_3$	1000 °C	770 °C	1520 °C
$ZrCl_4$	990 °C	770 °C	1500 °C
$HfCl_4$	970 °C	770 °C	1470 °C
VCl_3	1270 °C	900 °C	> 1935 °C
$NbCl_5$	1490 °C	1040 °C	> 1935 °C
$TaCl_5$	1420 °C	1000 °C	> 1935 °C
$CrCl_2$	1210 °C	860 °C	1900 °C
$CrCl_3$	1310 °C	930 °C	> 1935 °C
$MoCl_3$	1500 °C	1130 °C	> 1935 °C
$MoCl_5$	1500 °C	1250 °C	> 1935 °C
WCl_4	1500 °C	1230 °C	> 1935 °C
WCl_6	1500 °C	1280 °C	> 1935 °C
$ScCl_3$		520 °C	
YCl_3		460 °C	
$LaCl_3$		320 °C	
$MnCl_2$		770 °C	
$FeCl_2$		980 °C	
$FeCl_3$		1140 °C	
$CoCl_2$		1040 °C	
$NiCl_2$		1050 °C	

Table S4. Adiabatic temperatures for SSM reactions with KC_4 and KC_8. The determination of the adiabatic temperature is done graphically: T_{ad} is the temperature of the system when its enthalpy corresponds to the enthalpy of the reagents before reaction. KCl melts at 770 °C and boils at 1500 °C. $CaCl_2$ melts at 772 °C and boils at 1935 °C.

B.4. Powder X-ray diffractograms

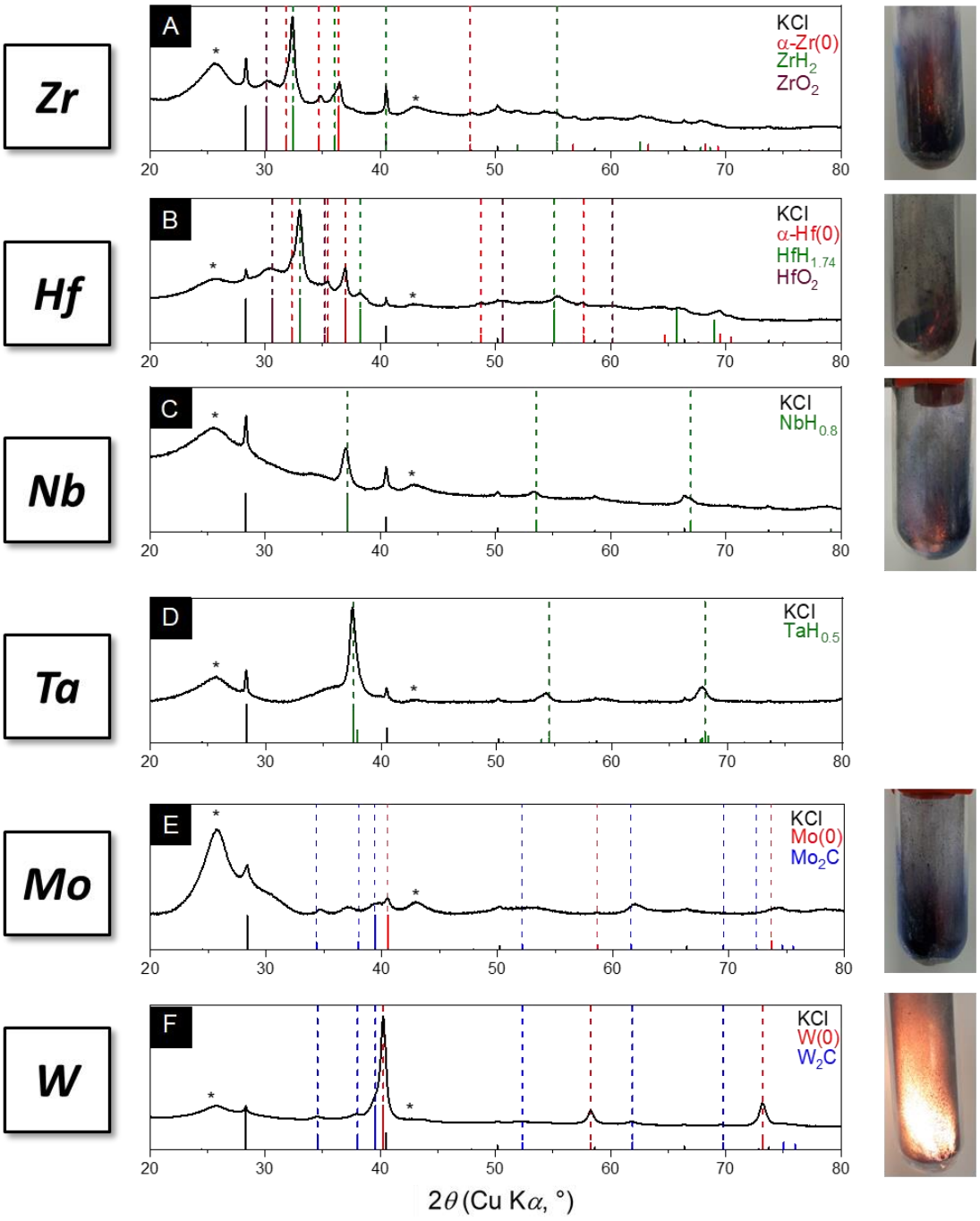

Figure S3: Snapshots of the explosion and PXRD patterns of washed powders obtained by reaction between KC_4 and metal chlorides when reaction is performed under vacuum: (A) $ZrCl_4$, (B) $HfCl_4$, (C) $NbCl_5$, (D) $TaCl_5$, (E) $MoCl_5$, (F) WCl_6.

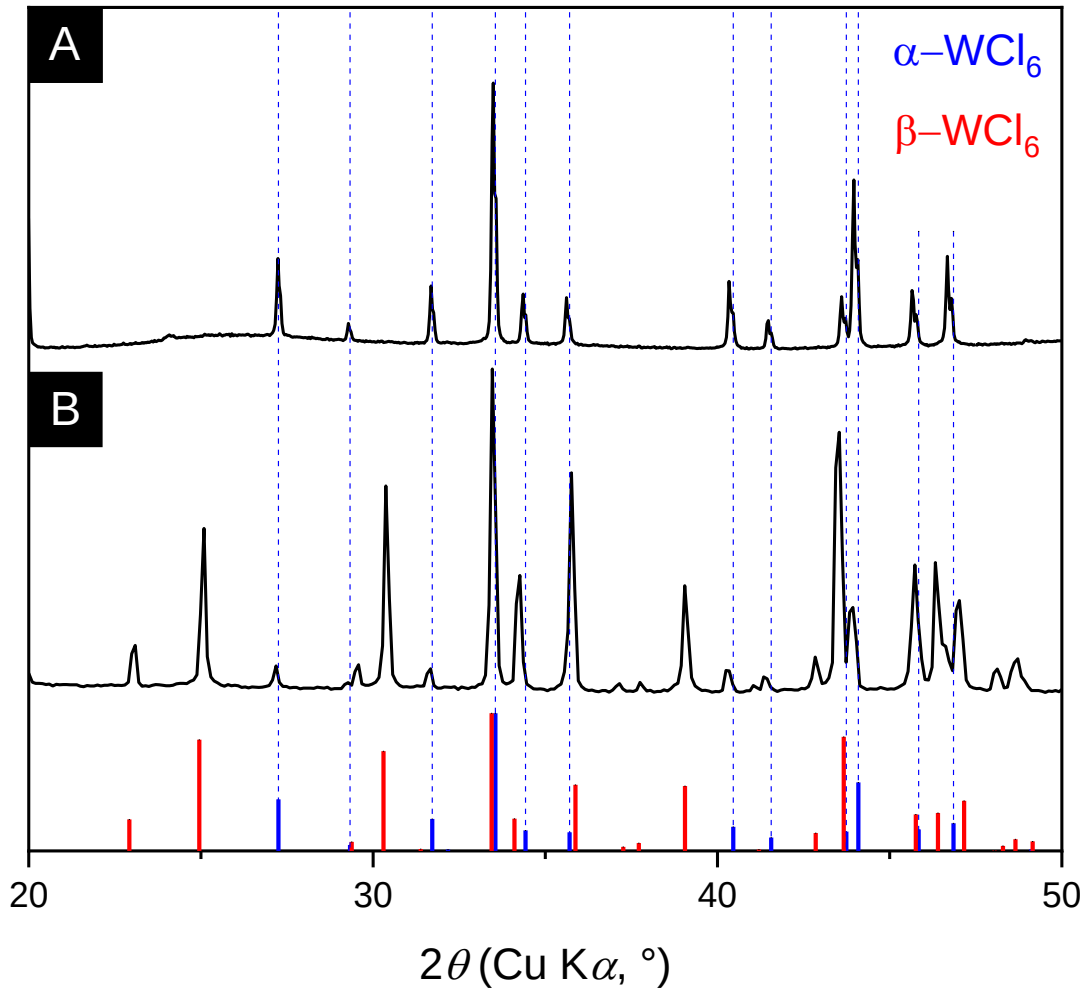

Figure S4: PXRD pattern of (A) commercial WCl_6 and (B) recrystallized sample (210 °C under vacuum).

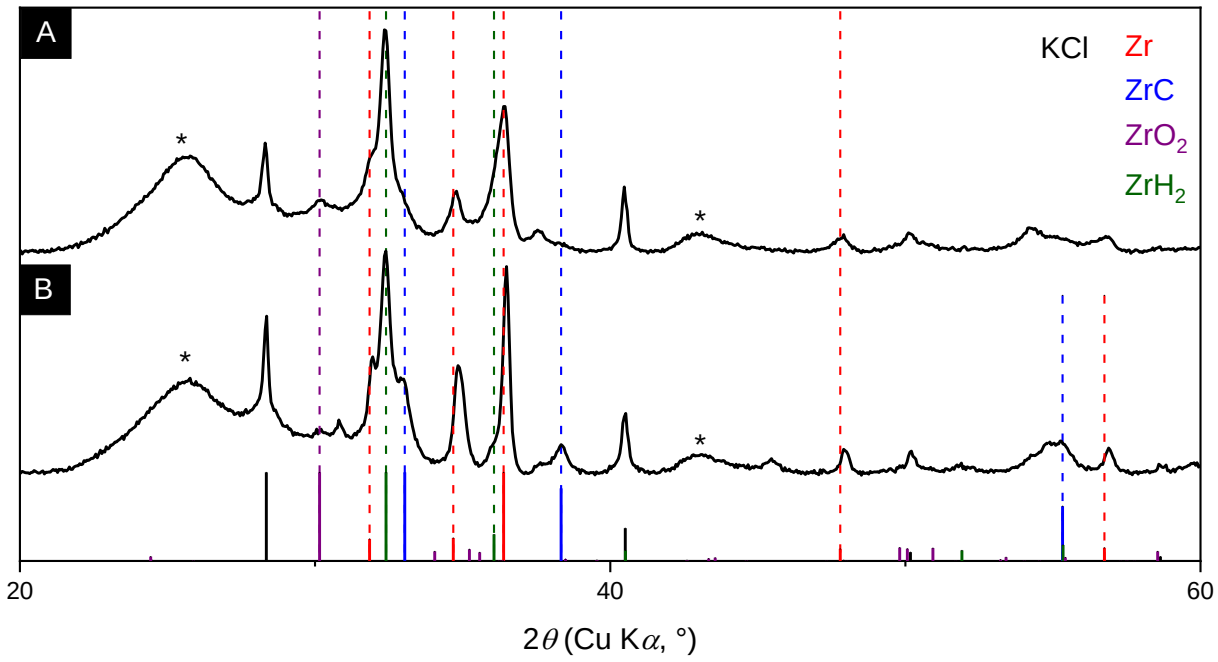

Figure S5: PXRD patterns of powders obtained by reaction between $ZrCl_4$ and 4 KC_4 (A) under vacuum and (B) in Ar. Stars correspond to acetylene black diffraction peaks.

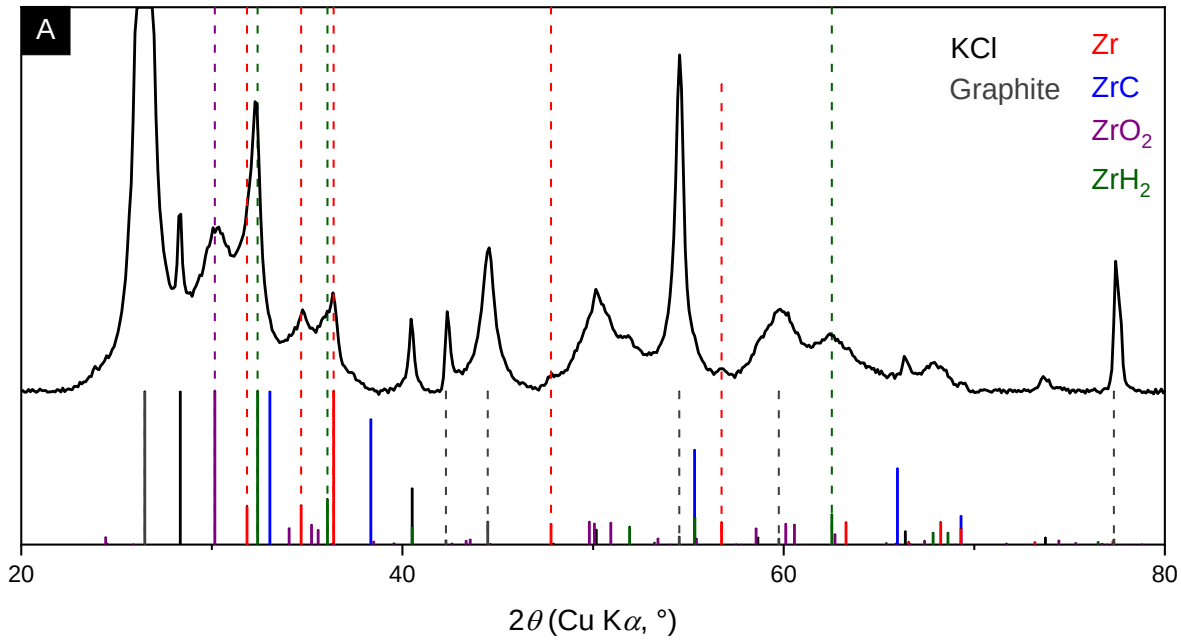

Figure S6: PXRD patterns of powders obtained by reaction between $ZrCl_4$ and 4 KC_8 under vacuum.

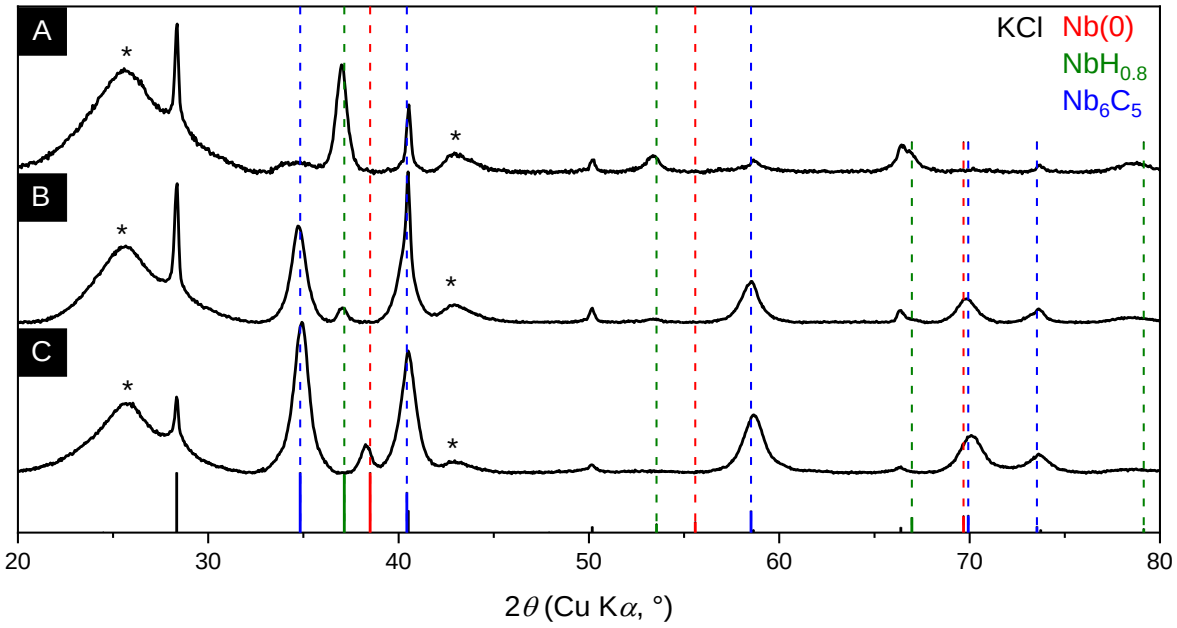

Figure S7: PXRD patterns of powders obtained by reaction between $NbCl_5$ and 4 KC_4 (A) under vacuum, (B) in Ar or (C) in N_2. Stars correspond to acetylene black diffraction peaks.

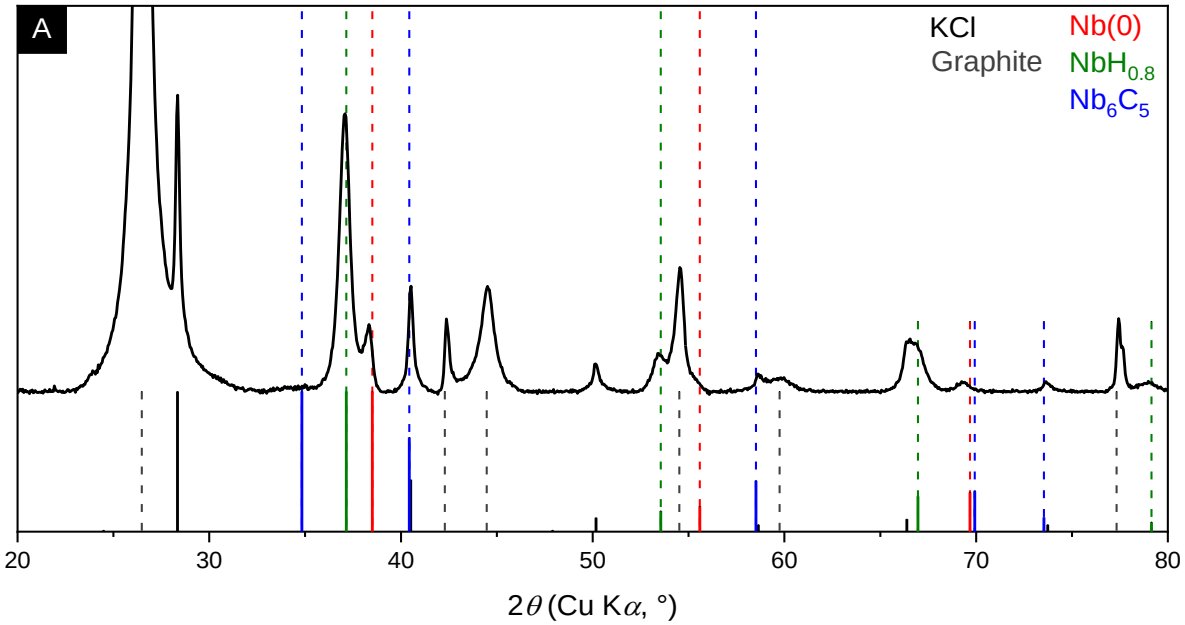

Figure S8: PXRD patterns of powders obtained by reaction between $NbCl_5$ and 4 KC_8 under vacuum.

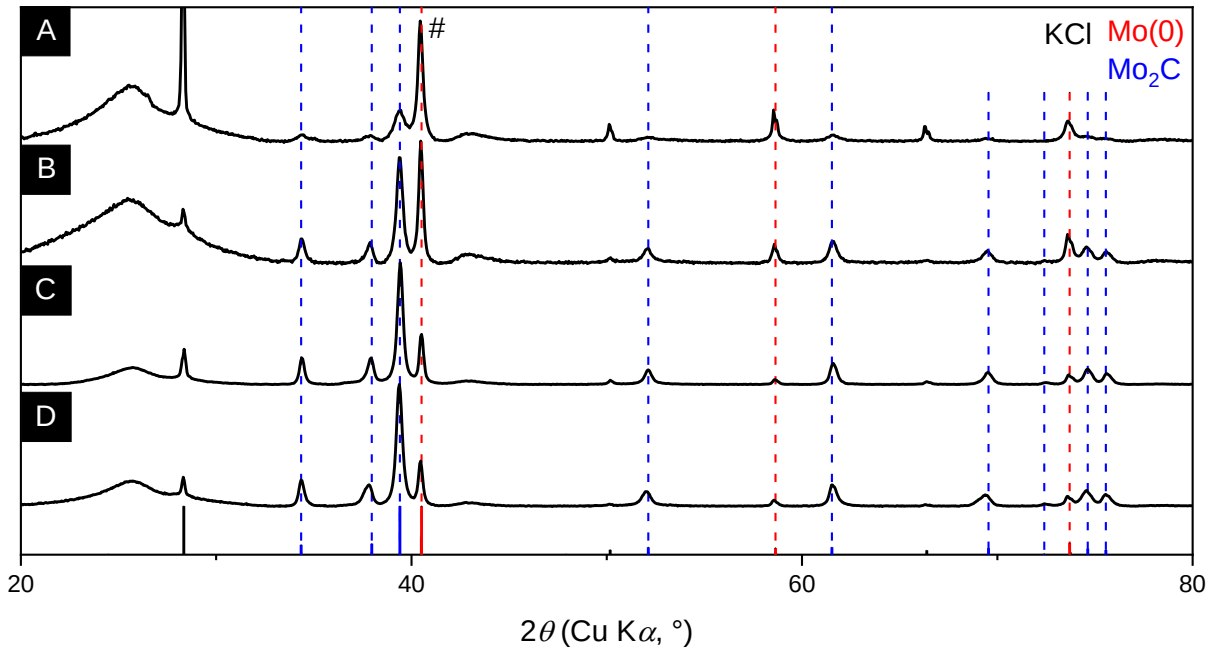

Figure S9: PXRD patterns of powders obtained by reaction between $MoCl_5$ and 5 KC_4 (A) under vacuum with coarse $MoCl_5$ grains (# peak contains a strong contribution of KCl), (B) in Ar, (C) in Ar with coarse $MoCl_5$ grains and (D) in N_2.

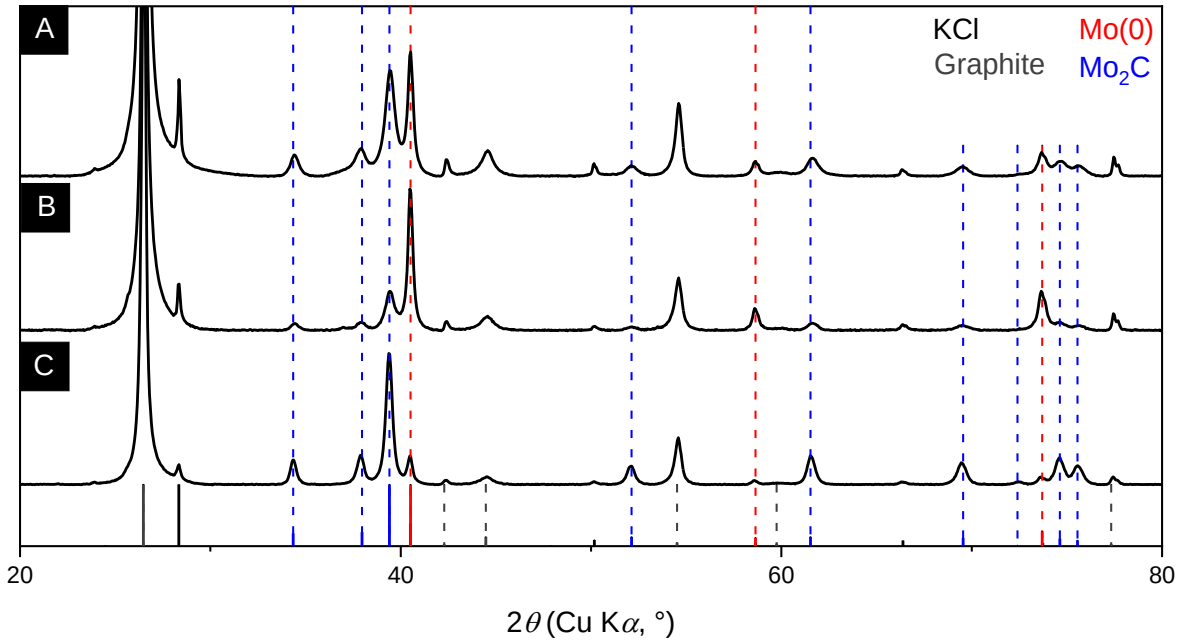

Figure S10: PXRD patterns of powders obtained by reaction between $MoCl_5$ and 5 KC_8 (A) under vacuum, (B) under vacuum with coarse $MoCl_5$ grains and (C) in Ar.

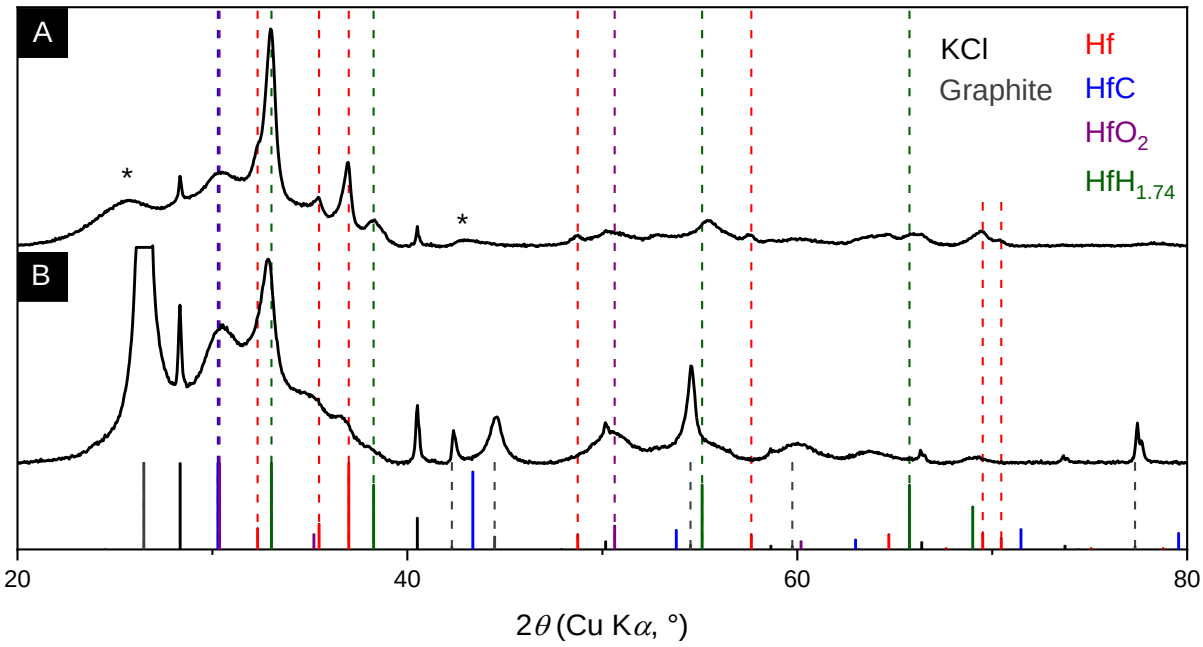

Figure S11: PXRD patterns of powders obtained by reaction between $HfCl_4$ and (A) 4 KC_4 or (B) 4 KC_8, both reactions under vacuum. Stars correspond to acetylene black diffraction peaks.

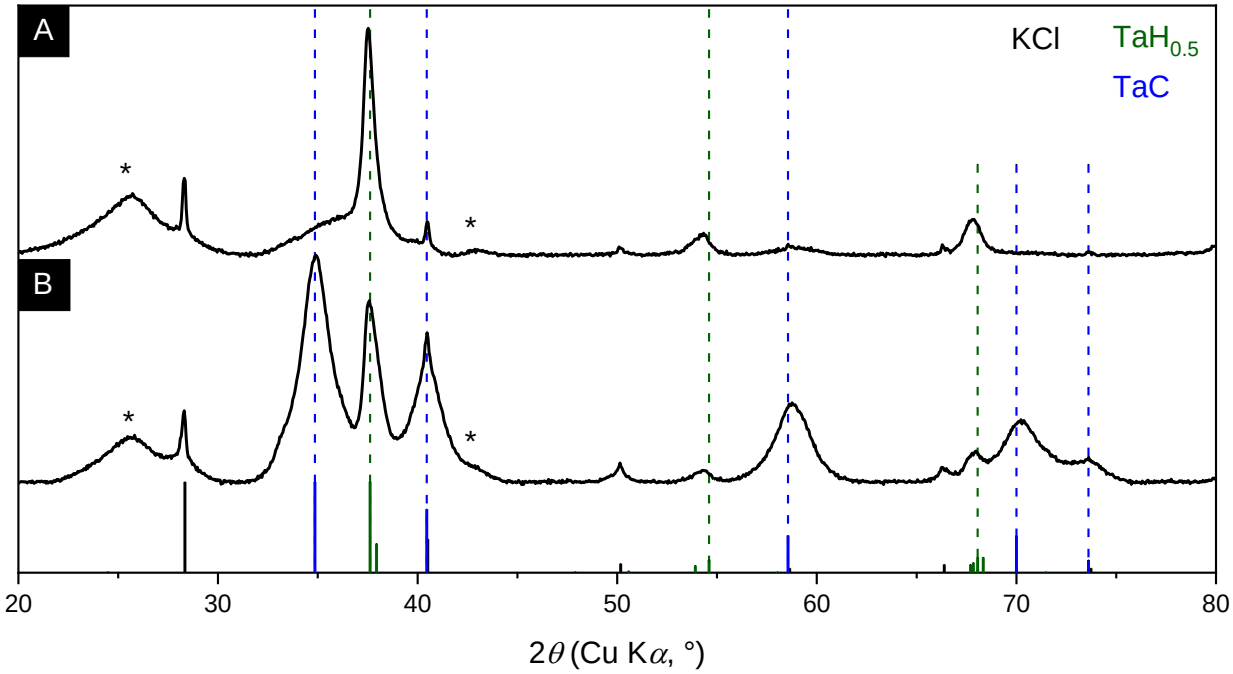

Figure S12: PXRD patterns of powders obtained by reaction between $TaCl_5$ and 5 KC_4 (A) under vacuum or (B) in Ar. Stars correspond to acetylene black diffraction peaks.

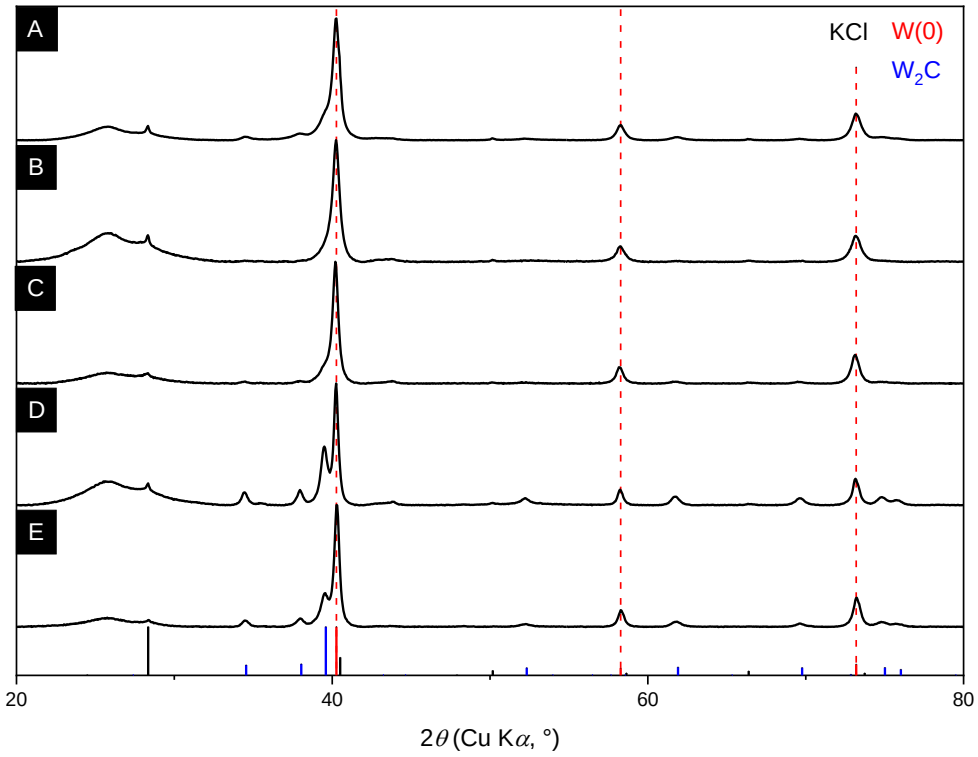

Figure S13: PXRD patterns of powders obtained by reaction between WCl_6 and 6 KC_4 (A) under vacuum, (B) under vacuum with coarse WCl_6 grains, (C) under vacuum with ground WCl_6 grains, (D) in Ar or (E) in N_2.

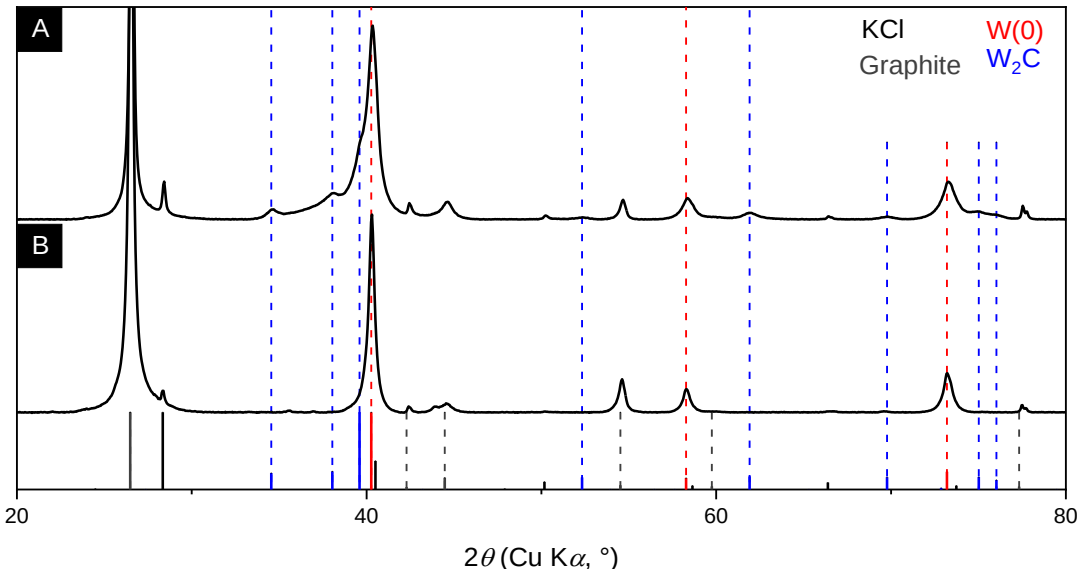

Figure S14: PXRD patterns of powders obtained by reaction between WCl_6 and 6 KC_8 under vacuum (A) with a fine powder of WCl_6 or (B) with coarse WCl_6 grains.

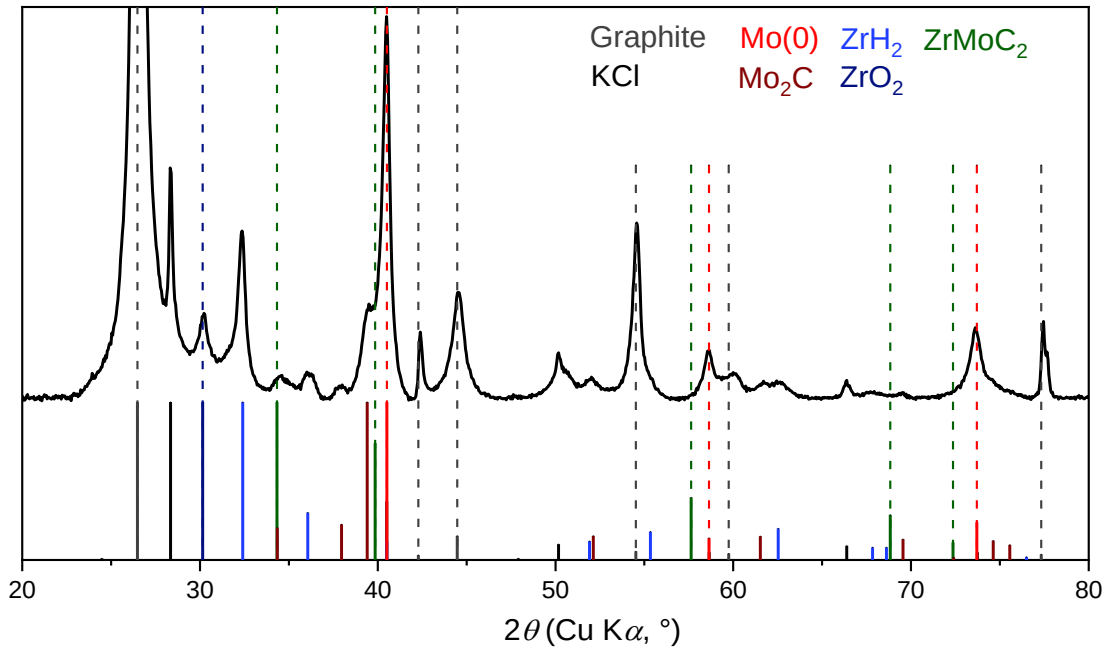

Figure S15: PXRD pattern of the product of the reaction with a stoichiometric mixture ($ZrCl_4$ + $MoCl_5$ + 9 KC_8) performed under vacuum.

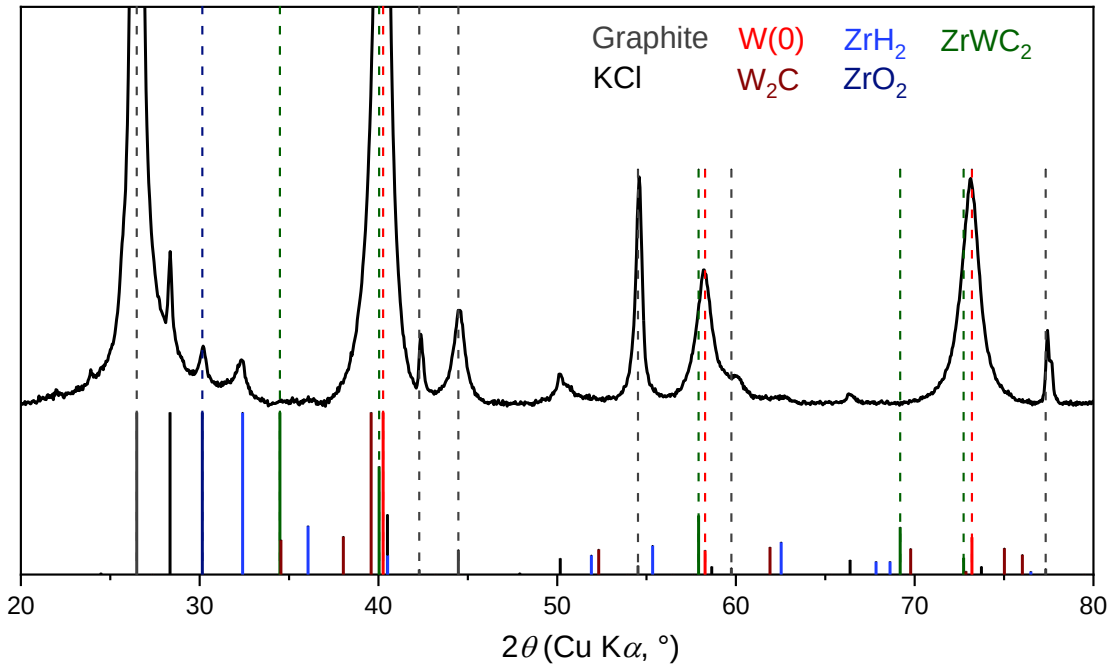

Figure S16: PXRD pattern of the product of the reaction with a stoichiometric mixture ($ZrCl_4$ + WCl_6 + 10 KC_8) performed under vacuum.

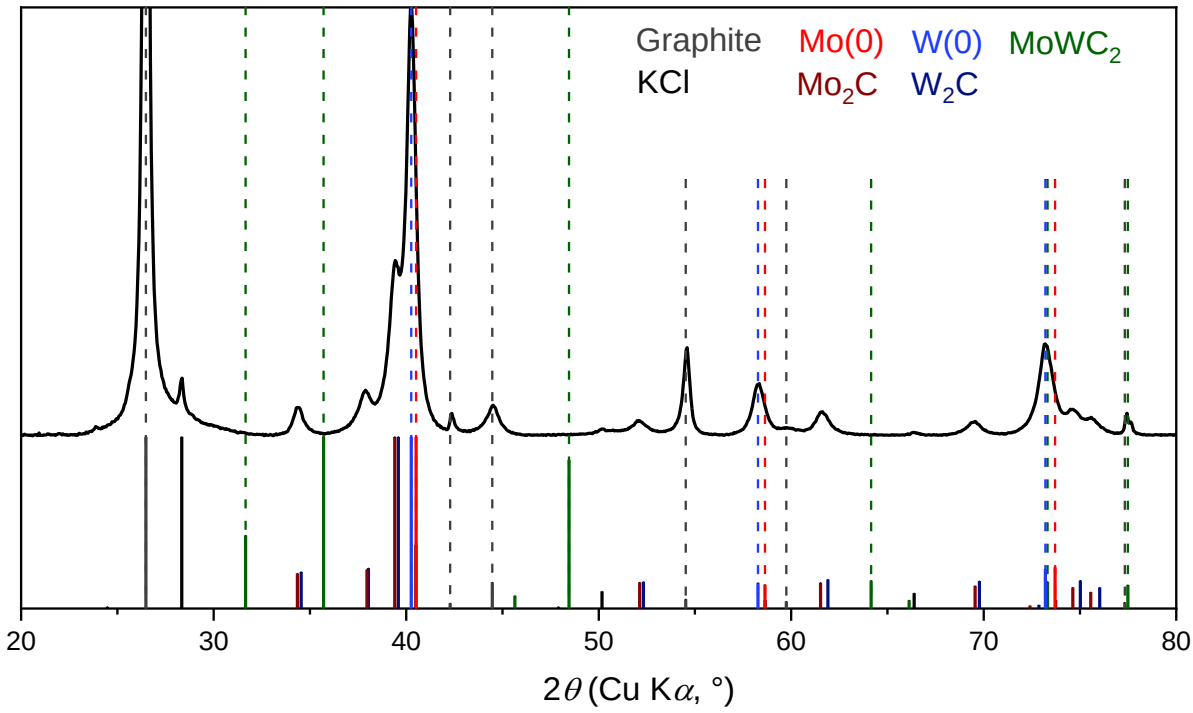

Figure S17: PXRD pattern of the product of the reaction with a stoichiometric mixture ($MoCl_5$ + WCl_6 + 11 KC_8) performed under vacuum.

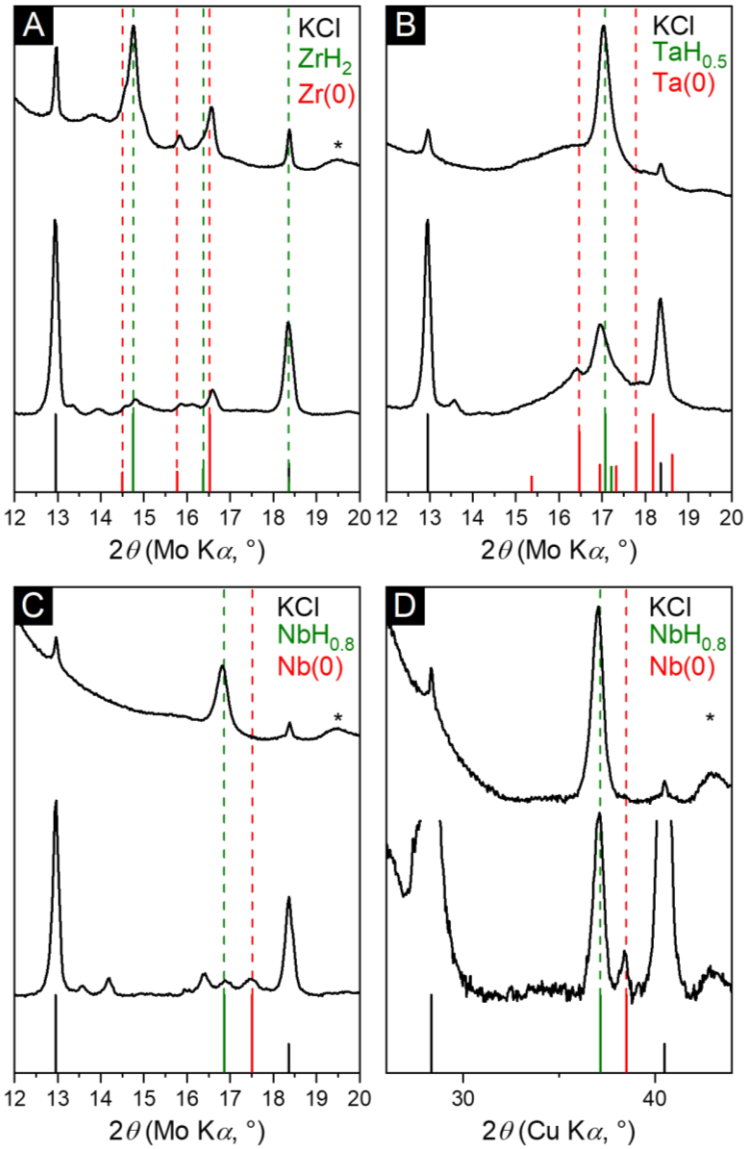

Figure S18: PXRD pattern of the product of the reaction with a stoichiometric mixture $MCl_x + x\,KC_4$ performed under vacuum. (A) $ZrCl_4$, after neutralization (top) and before neutralization under Ar in capillary (bottom). (B) $TaCl_5$, after neutralization (top) and before neutralization under Ar in capillary (bottom). (C) $NbCl_5$, after neutralization (top) and before neutralization under Ar in capillary (bottom). (D) $NbCl_5$ after neutralization with EtOH and water (top) and before neutralization after exposure to air (bottom).

B.5. TEM images

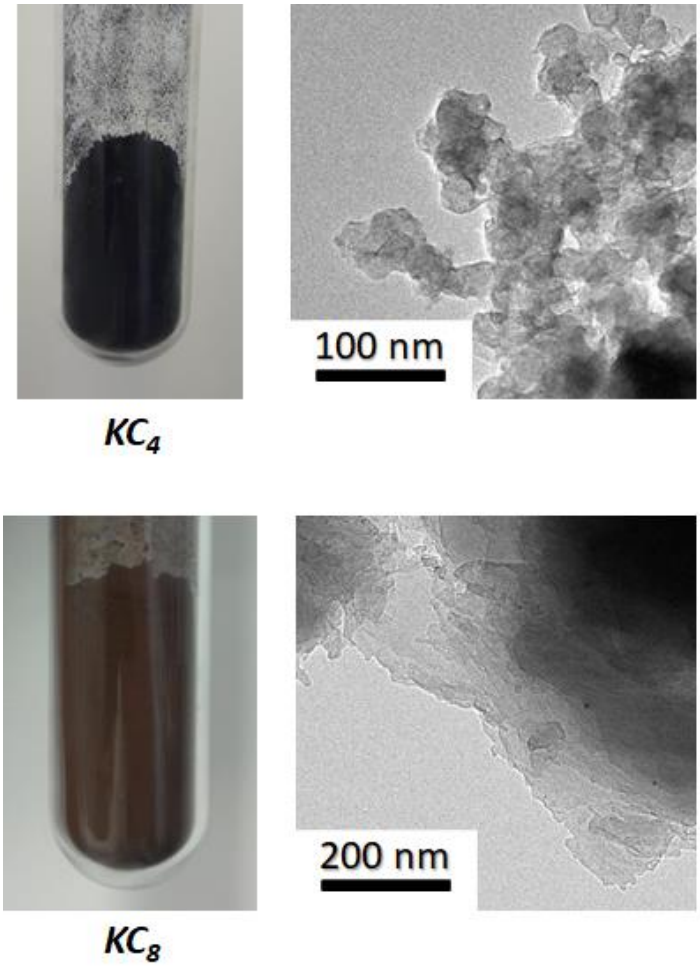

Figure S19: Pictures of potassium dispersed in carbon and TEM images of the corresponding carbon phase without potassium (top: KC_4 and acetylene black, bottom: KC_8 and graphite).

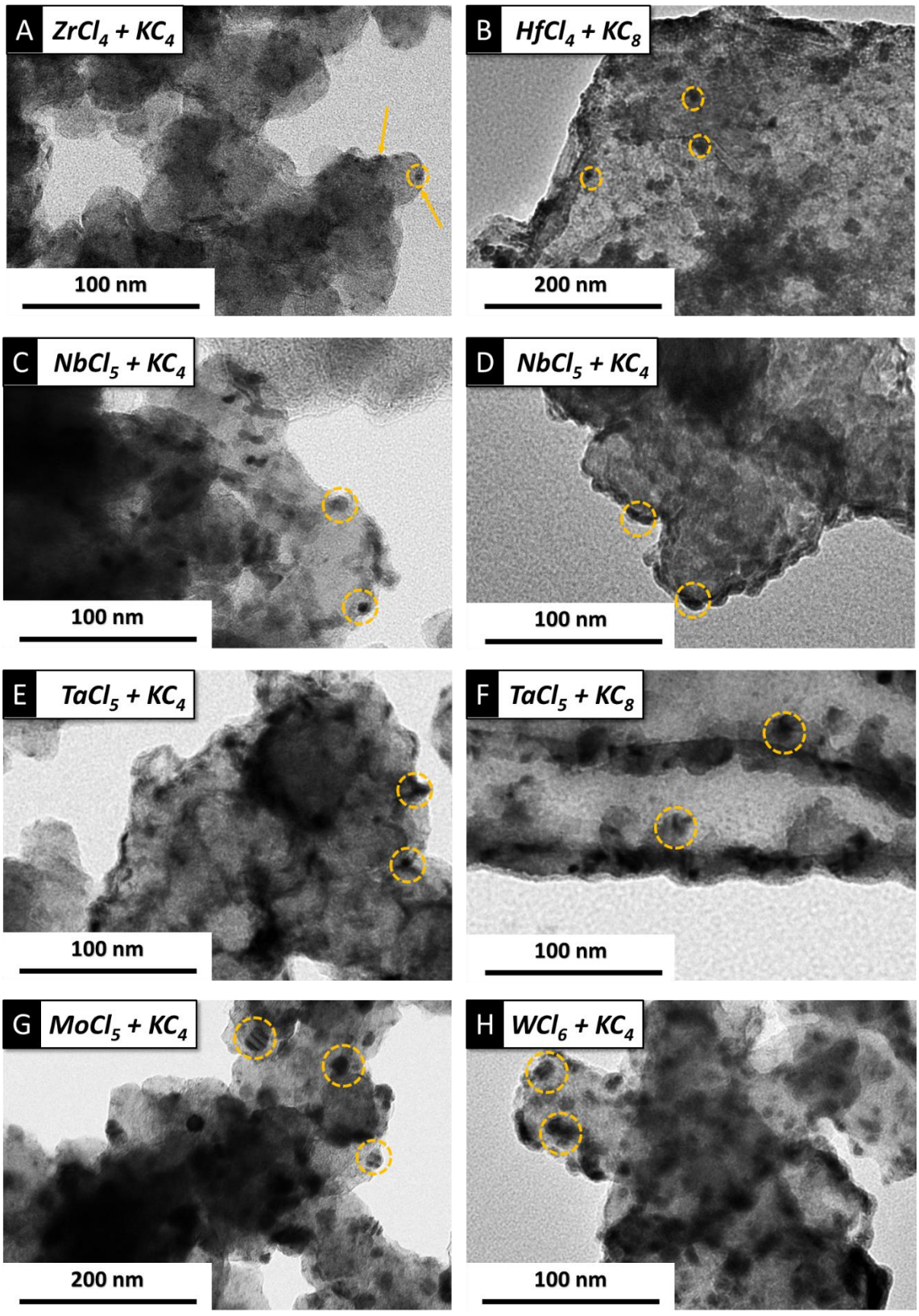

Figure S20: TEM images of different particles supported on carbon supports from reaction between KC_4/KC_8 and metal chlorides

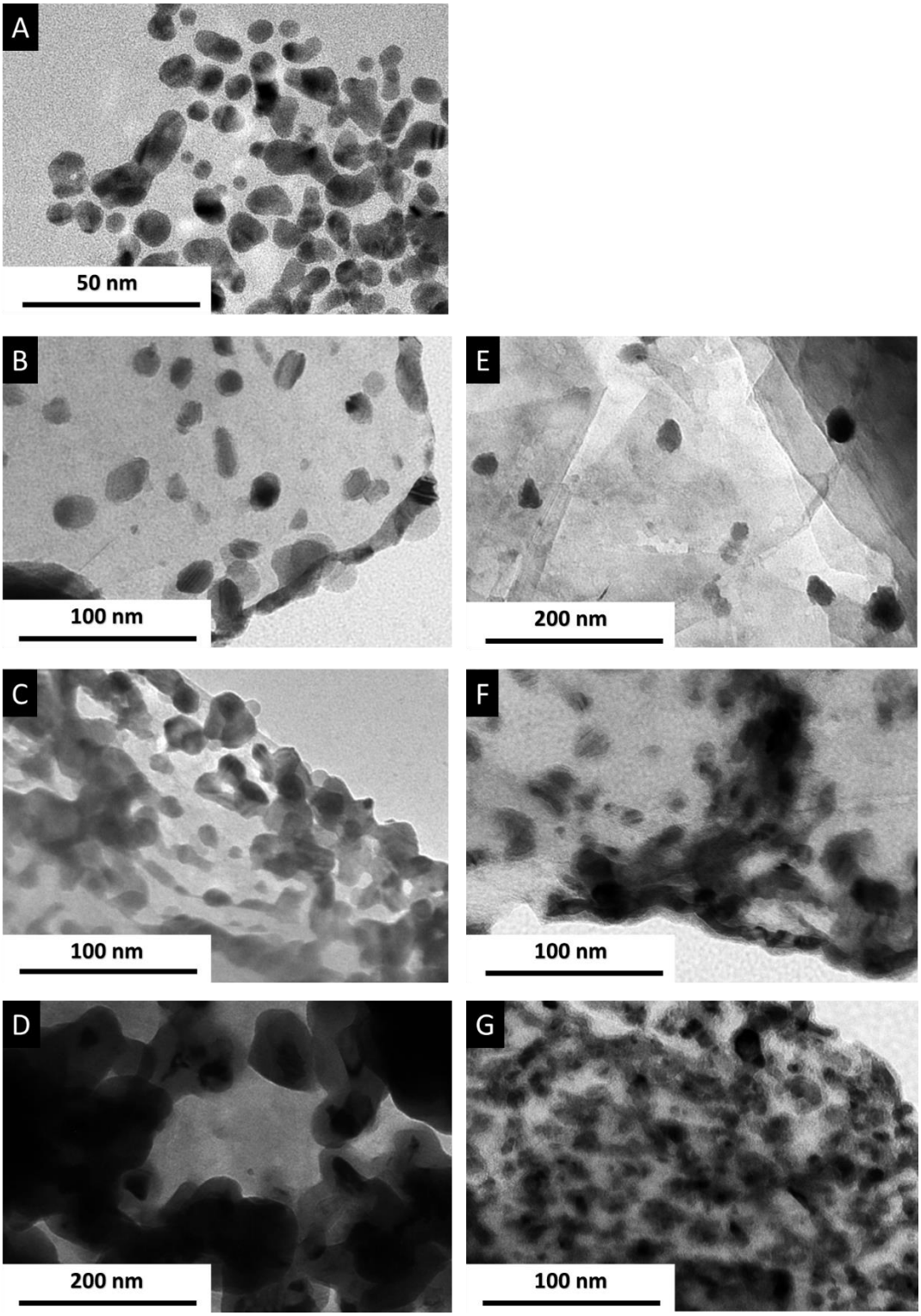

Figure S21: TEM images of particles supported on graphite from reaction between KC_8 and (A-D) $MoCl_5$ or (E-G) WCl_6.

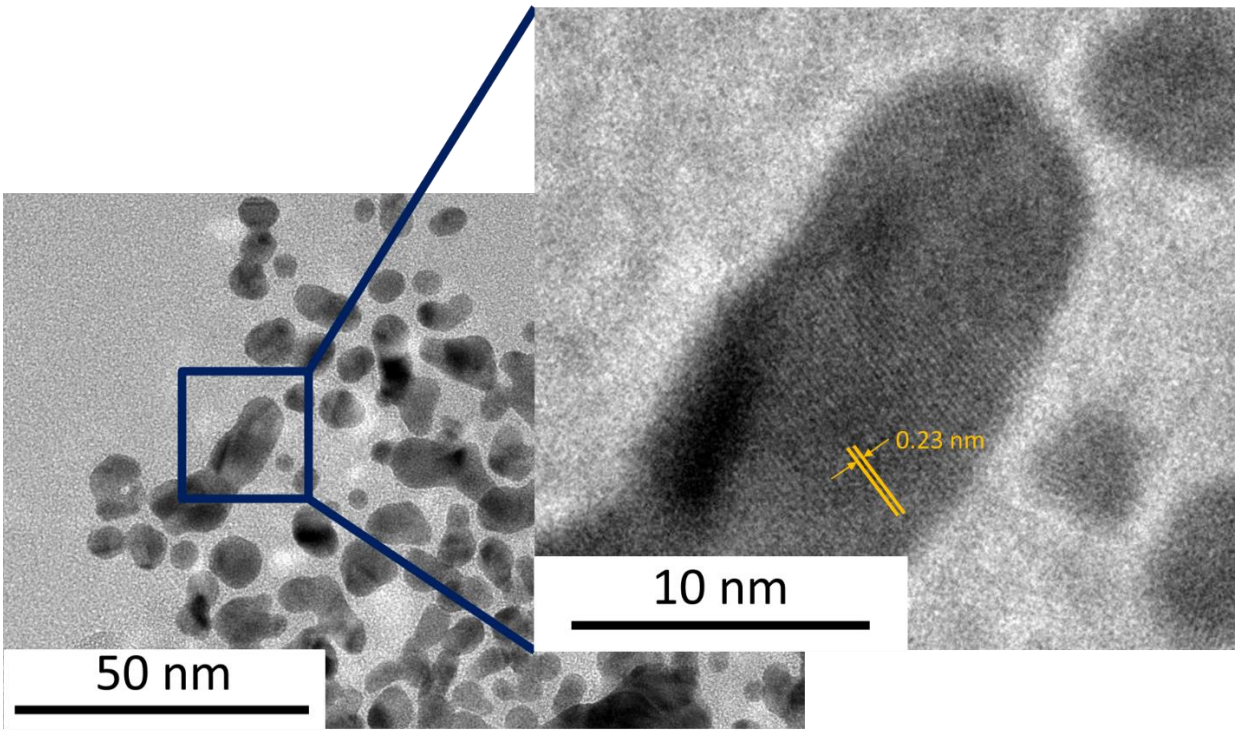

Figure S22. Transmission Electron Microscopy image of free molybdenum carbide nanoparticles. Details of crystal fringes (0.23 nm observed in TEM, Mo_2C has a diffraction peak at 0.228 nm)

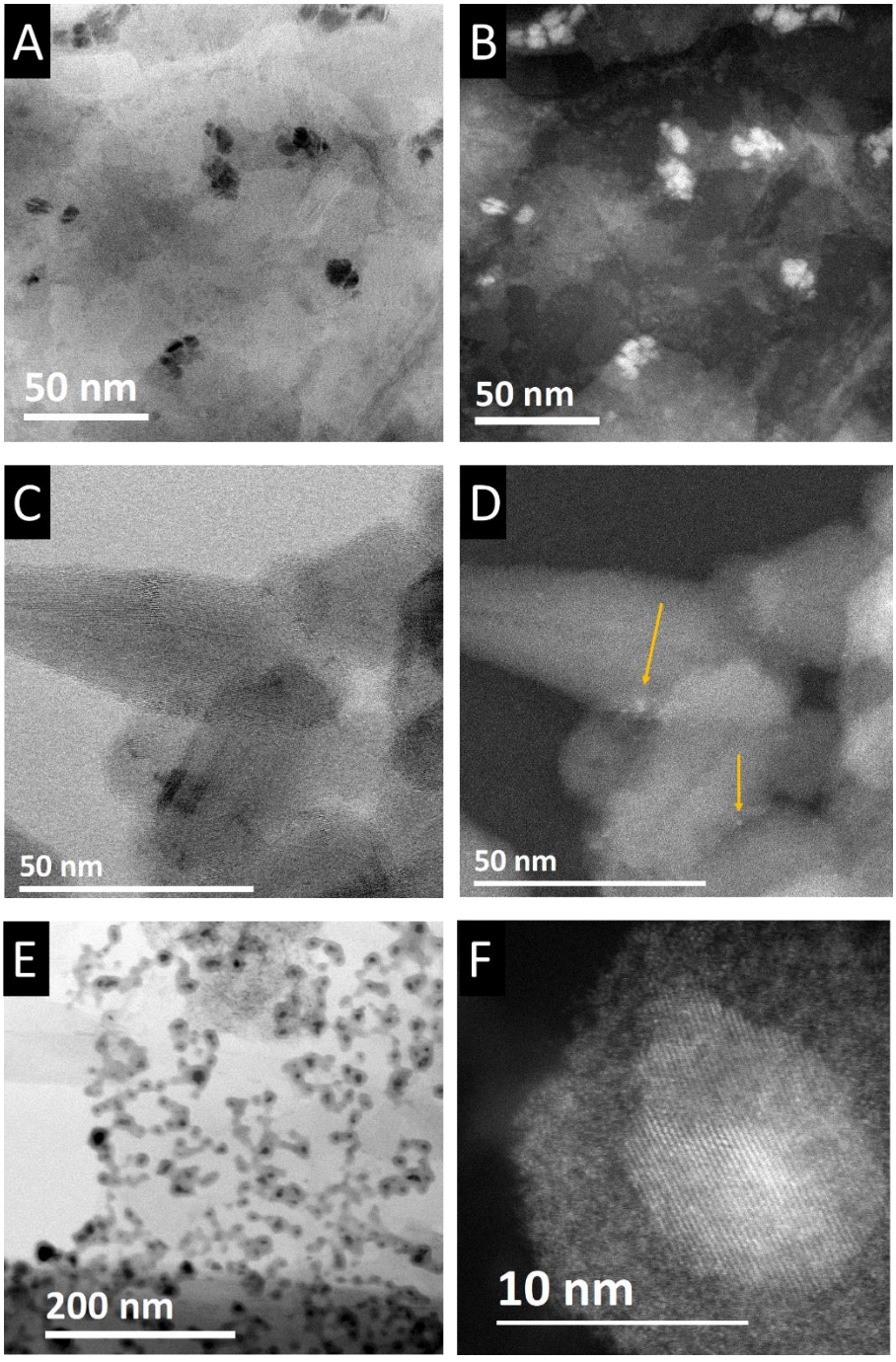

Figure S23. Bright Field (BF, left) and Dark Field (DF, right)) High Resolution Scanning Transmission Electron Microscopy (HRSTEM) image of clusters/small particles containing (A-B) molybdenum or (C-D) tungsten atoms. (E-F) Tungsten-containing core-shell particles.

B.6. SEM and EDXS measurements

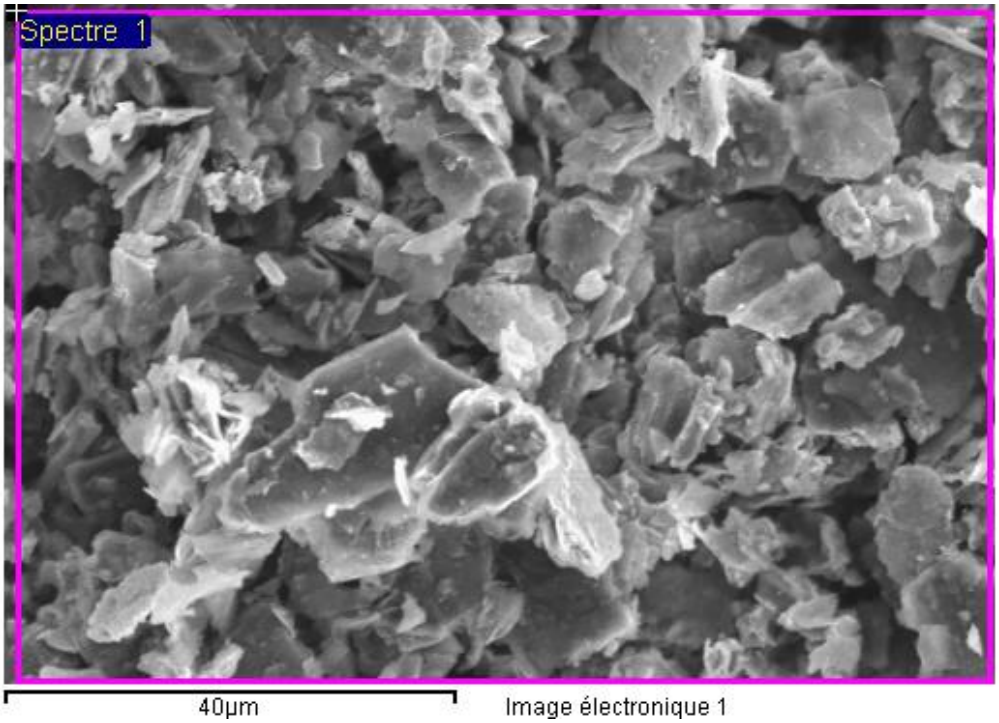

Figure S24: Scanning Electron Microscopy image of the product of the reaction performed on WCl_6 + 6 KC_8.

Zone	Zr (mol. %)	Mo (mol. %)	K (mol. %)	Cl (mol. %)	Molar ratio Zr/Mo
1	15.9	16.4	9.2	10.2	0.97
2	15.4	16.4	9.3	9.6	0.94
3	26.6	12.7	7.5	8.3	2.10
4	16.7	17.6	7.9	8.1	0.95
5	16.5	13.6	10.3	8.7	1.21
6	15.5	22.8	7.9	7.9	0.68
Average	17.8 ± 2.1	16.6 ± 1.9	8.7 ± 1	8.8 ± 1	1.1

Table S5: EDS on different zones of the product of reaction performed on $ZrCl_4$ + $MoCl_5$ + 9 KC_8.

Zone	Zr (mol. %)	W (mol. %)	K (mol. %)	Cl (mol. %)	Molar ratio Zr/W
1	17	20.6	8.6	10	0.83
2	19.4	23	5.6	6.4	0.84
3	18	17.9	8.2	9	1.00
4	18.3	18.9	8.4	7.8	0.97
5	17.7	20	8.7	8	0.88
6	17.1	17.6	8.8	9.4	0.97
7	18.1	19	8.1	9.3	0.95
Average	17.9 ± 0.9	19.6 ± 1.4	8.0 ± 1	8.5 ± 1.1	0.9

Table S6: EDS on different zones of the product of reaction performed on $ZrCl_4$ + WCl_6 + 10 KC_8.

Zone	Mo (mol. %)	W (mol. %)	K (mol. %)	Cl (mol. %)	Molar ratio Mo/W
1	17.3	17.1	12.4	10.3	1.01
2	14.7	19.7	13.7	11.2	0.75
3	19.3	19.0	10.1	8.0	1.02
4	21.1	21.1	12.8	8.9	1
5	18.4	22.8	10.3	7.9	0.81
Average	18.2 ± 1.5	19.9 ± 1.5	11.9 ± 1.3	9.3 ± 1.2	0.9

Table S7: EDS on different zones of the product of reaction performed on $MoCl_5$ + WCl_6 + 11 KC_8.

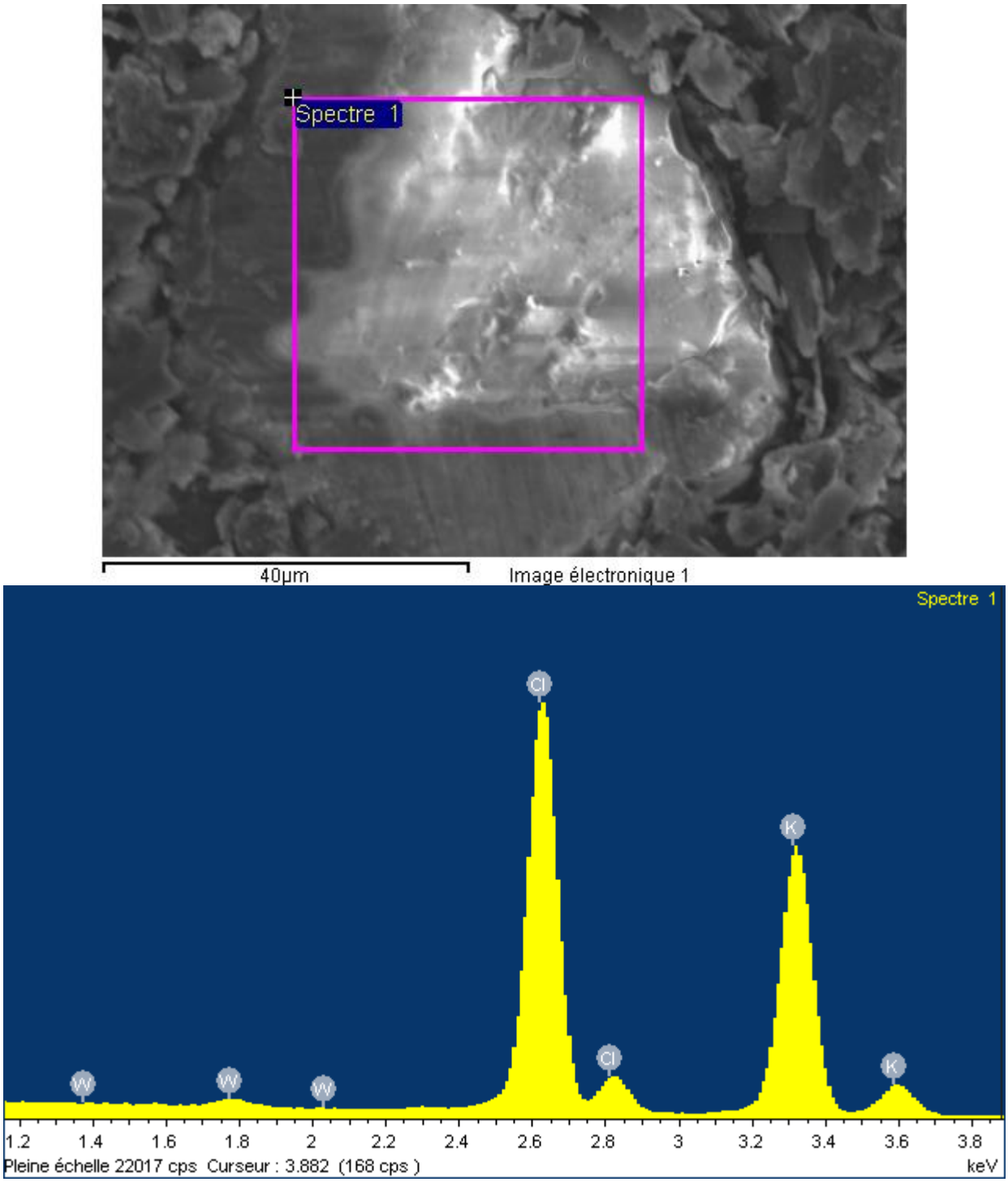

Figure S25: EDS of reaction performed on WCl_6 + $MoCl_5$ + 11 KC_8, zoom on a facetted micron-sized crystals of KCl.

B.7. X-ray Photoelectron Spectroscopy

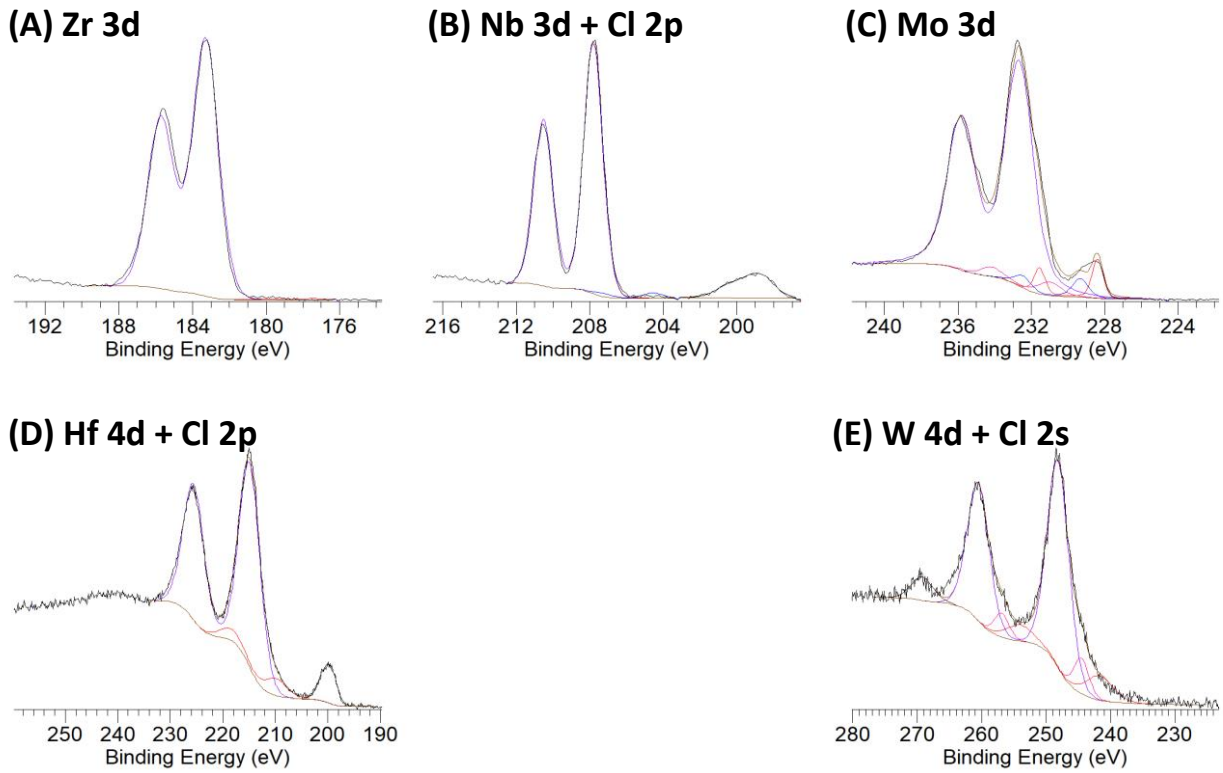

Figure S26: XPS spectra of **d** regions of metal for reactions performed with MCl_x + x KC_4. (A) Zr 3d, (B) Nb 4d, (C) Mo 3d, (D) Hf 4d and (E) W 4d. Nb 3d, Hf 4d and W 4d regions also contain signal from Cl atoms coming from residual KCl. The contributions have been plotted on each subfigure: in red, contribution of the M(0) species, in blue, contribution of the M(+II) species, and in magenta, contribution of the M(+IV) species (for Mo 4d and W 4d), in purple, contribution of the most oxidized species.

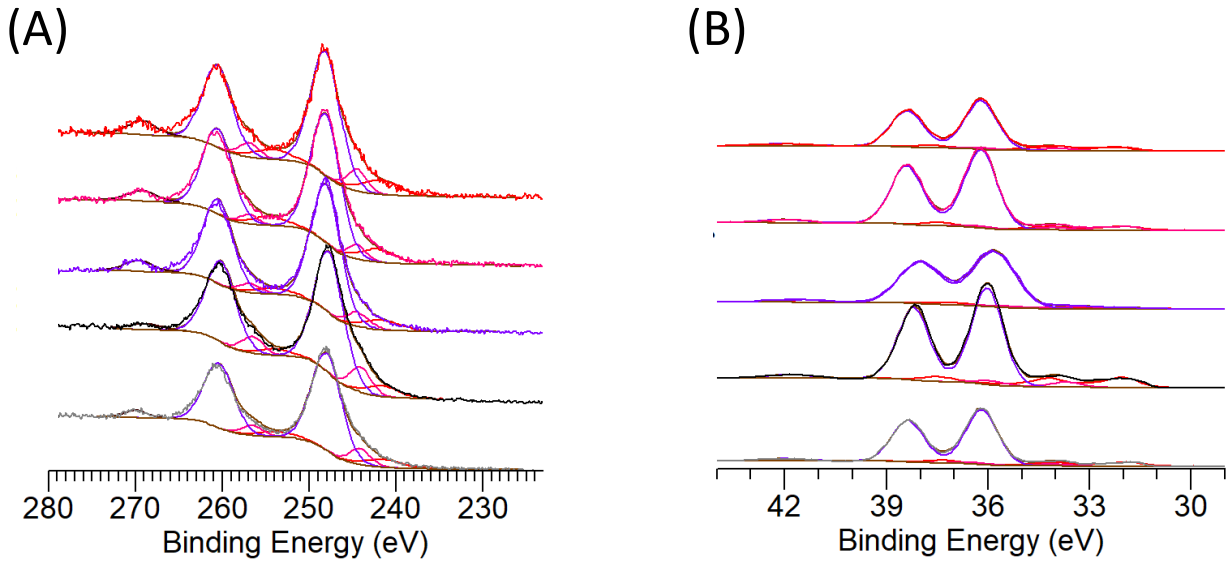

Figure S27: XPS spectra of the (A) W **4d** and (B) W **4f** region of samples obtained from the reaction between WCl_6 and KC_4 or KC_8 with different process parameters (carbon source, atmosphere and metal chloride granularity). From top to bottom: KC4_vacuum_fine grains (red spectrum), KC4_Ar_fine grains (magenta spectrum), KC4_vacuum_coarse grains (purple spectrum), KC8_vacuum_fine grains (black spectrum), KC8_vacuum_coarse (grey spectrum). For each sample, the contributions are: red: W(0), magenta: W(+IV), purple: W(+VI), black: residue of Cl 2s.

C. References

[1] D. Ressnig, S. Moldovan, O. Ersen, P. Beaunier, D. Portehault, C. Sanchez, S. Carenco, *Chem. Commun.* **2016**, *52*, 9546–9549.

[2] A. M. Nartowski, I. P. Parkin, A. J. Craven, M. MacKenzie, *Adv. Mater.* **1998**, *10*, 805–808.

[3] A. M. Nartowski, I. P. Parkin, M. MacKenzie, A. J. Craven, I. MacLeod, *J. Mater. Chem.* **1999**, *9*, 1275–1281.

[4] A. M. Nartowski, I. P. Parkin, M. Mackenzie, A. J. Craven, *J. Mater. Chem.* **2001**, *11*, 3116–3119.

[5] Y.-H. Chang, C.-W. Chiu, Y.-C. Chen, C.-C. Wu, C.-P. Tsai, J.-L. Wang, H.-T. Chiu, *J. Mater. Chem.* **2002**, *12*, 2189–2191.

[6] K. Gibson, M. Ströbele, B. Blaschkowski, J. Glaser, M. Weisser, R. Srinivasan, H.-J. Kolb, H.-J. Meyer, *Zeitschrift für Anorg. und Allg. Chemie* **2003**, *629*, 1863–1870.

[7] X. Feng, Y.-J. Bai, B. Lü, C.-G. Wang, Y.-X. Liu, G.-L. Geng, L. Li, *J. Cryst. Growth* **2004**, *264*, 316–319.

[8] J. D. Newell, S. N. Patankar, *Mater. Lett.* **2009**, *63*, 81–83.

[9] L. Wang, Q. Li, Y. Zhu, Y. Qian, *Int. J. Refract. Met. Hard Mater.* **2012**, *31*, 288–292.

[10] L. Wang, L. Si, Y. Zhu, Y. Qian, *Int. J. Refract. Met. Hard Mater.* **2013**, *38*, 134–136.

[11] L. WANG, W. XI, T. MEI, Y. CAI, J. LU, D. ZHAO, H. HUANG, W. LIU, Q. ZHOU, *J. Ceram. Soc. Japan* **2017**, *125*, 789–791.

[12] C. Guo, Y. Liu, X. Ma, Y. Qian, L. Xu, *Chem. Lett.* **2006**, *35*, 1210–1211.

[13] M. Lei, H. Z. Zhao, H. Yang, B. Song, W. H. Tang, *J. Eur. Ceram. Soc.* **2008**, *28*, 1671–1677.

[14] P. G. Li, M. Lei, W. H. Tang, *Mater. Res. Bull.* **2008**, *43*, 3621–3626.

[15] M. W. Chase, *NIST-JANAF Thermochemical Tables, 4th Edition*, **1998**.

[16] A. T. D. Butland, R. J. Maddison, *J. Nucl. Mater.* **1973**, *49*, 45–56.